Arch. Metall. Mater. **71** (2026), 1, 411-418

DOI: https://doi.org/10.24425/amm.2026.157803

DONGDONG SONG[1,2], XIANGJUN LIU[1,2], XIAOBIN JIA[3], MINGYI ZHANG[4],
LEI REN[1,2], CHANGQIAO YANG[1,2*]

NUMERICAL SIMULATION STUDY ON MOVEMENT BEHAVIOR OF RARE EARTH INCLUSIONS IN DIE STEEL AT MOLTEN STEEL-SLAG INTERFACE

Rare earth (RE) has a significant metamorphic effect on inclusions in steel, but there are few systematic analyses on the floating behavior of RE inclusions in molten metal. In this work, electroslag remelting die steel was taken as the research object, the separation process of RE inclusions at the molten steel-slag interface (MSSI) was discussed by mathematical model. The results show that the floating movement of RE inclusions in molten steel belongs to Stokes flow. The size of RE inclusions has a significant effect on the time it takes to pass through MSSI, and the larger the inclusion, the longer the time required. In addition, the movement displacement of RE inclusions passing through MSSI is restricted by the surface tension between steel and slag, and a higher surface tension can reduce the movement displacement of RE inclusions, which is not conducive for RE inclusions to pass through the interface. Furthermore, the slag density has little influence on the velocity of RE inclusion passing through MSSI.

Keywords: Rare earth inclusions; Steel-slag interface; Reynolds number; Mathematical model

1. Introduction

Inclusions are heterogeneous substance in steel matrix, which will destroy the continuity of the steel matrix and deteriorate the mechanical properties and corrosion resistance of steel. It is the key to producing high-quality steel whether inclusions can be effectively removed. Inclusions can be removed by refractory absorption [1] and filter filtration [2] methods, top-slag absorption is recognized as the most significant and effective. The floating process of inclusions in molten metal consists of three phases: inclusions float up to MSSI, inclusions cross MSSI and into the slag layer, and inclusions dissolve in slag. Among them, the first step, the floating process acts as the momentum accumulation stage [3] before approaching the interface, and the third step, the inclusions are dissolved in the slag phase [4]. At present, these two stages have been extensively studied and some instructive conclusions have been drawn. However, there are relatively few studies on the second step.

The mathematical model is one of the most important tools to study metallurgical processes. Since 1992, when Nakajima et al. [5] created the first model of the movement of inclusions at MSSI, there have been continuous innovations and breakthroughs in this field, which have offered many new insights into the movement of inclusions and the optimization of clean steel smelting processes. Considering the combined effects of buoyancy, additional mass force, capillary force, and drag force on the movement of inclusions cross MSSI during the separation process, Strandh et al. [6,7] proposed a series of ideal hypotheses on the key problems in the removal process of inclusions, and created a motion model of inclusions separation mechanisms at MSSI. Yang et al. [8,9] considered the effect of Reynolds number (Re), and modified the above mathematical model. They selected an appropriate model based on a larger range of Re, and obtained the displacement curve of inclusions over time. Tao et al. [10] established a water model experiment system using silicone oil to simulate slag phase and alumina particles to represent non-metallic inclusions by combining mathematical modeling and physical simulation, and analyzed the influence of key parameters such as slag viscosity and inclusion particle size on the movement behavior of inclusions at the interface. Zhou et al. [11] found that existing mathematical models of the separation process neglected the influence of resistance at MSSI

[1] INNER MONGOLIA UNIVERSITY OF SCIENCE AND TECHNOLOGY, SCHOOL OF RARE EARTH INDUSTRY, BAOTOU 014010, INNER MONGOLIA, CHINA
[2] INNER MONGOLIA UNIVERSITY OF SCIENCE AND TECHNOLOGY, KEY LABORATORY OF GREEN EXTRACTION & EFFICIENT UTILIZATION OF LIGHT RARE-EARTH RESOURCES, MINISTRY OF EDUCATION, BAOTOU 014010, INNER MONGOLIA, CHINA
[3] INNER MONGOLIA NORTH HEAVY INDUSTRY GROUP CO., LTD., BAOTOU 014033, INNER MONGOLIA, CHINA
[4] INNER MONGOLIA INSTITUTE OF METAL MATERIALS, BAOTOU 014034, INNER MONGOLIA, CHINA

* Corresponding author: yangchangqiao@imust.edu.cn

and could not reasonably explain the physical simulation experiments. Therefore, the effects of Re and interface resistance must be considered when establishing a mathematical model of solid inclusions movement at MSSI.

Cao et al. [12] constructed a mathematical model covering the movement of inclusions, interfacial tension, and slag surface tension, and evaluated the ability of refining slag containing Ce_2O_3 to remove Al_2O_3 inclusions. The results showed that larger inclusions and lower slag viscosity are beneficial to the removal of inclusions. At present, it has been recognized that RE can effectively modify inclusions in steel [13-17]. After treatment with RE, the inclusions usually have spherical, nearly spherical, or elliptical shapes, and the comprehensive mechanical performance of the solidified steel have been markedly improved.

However, to the best of our knowledge, the systematic research on the movement behaviors of RE inclusions at MSSI has been conducted less. In this work, the effects of Re and interface resistance is considered, and the change rules of rare earth inclusions in the molten steel and at the molten steel-slag interface is analyzed, and a mathematical model for the separation of spherical rare earth inclusions at the molten steel-slag interface. Furthermore, the influence of different variables on the inclusions crossing MSSI is discussed.

2. Mathematical model

2.1. Model hypotheses

Non-metallic inclusions exhibit distinct movement behaviors when crossing MSSI due to their different properties. The inclusions under the RE slag system are usually solid inclusions, so this study mainly focused on solid inclusions [13]. During the floating of inclusions, MSSI is stable, and the vertical velocities of the nearby molten steel, slag, and solid inclusions are converted into the floating velocity of the inclusions. Based on the following hypotheses, a mathematical model of solid RE inclusions passing through MSSI is established.

(1) During separation process, the composition, shape, and size of the inclusions remain unchanged.
(2) During separation process, the chemical reactions between molten steel, slag, and inclusions are ignored.
(3) The interfacial tensions of different phases (steel, slag, and solid inclusions) are all constant.
(4) The rotational speed of the inclusions is 0.
(5) Since the size of inclusions is very small, the pressure of molten steel on the inclusion surface is assumed to be the same, and the velocity gradient of steel around the inclusions is 0. In other words, the influence of horizontal steel and slag flow on inclusions passing through MSSI is ignored.
(6) The model assumes that the initial velocity of inclusions impacting the interface is the limiting floating velocity.
(7) The shape of the inclusions is spherical.

2.2. Equations of motion

2.2.1. Selection of floating terminal velocity of inclusions

The inclusions are subjected to a drag force of steel during the floating process, and the magnitude of the drag force is related to the floating velocity of inclusions. Due to the accelerating effect of buoyancy of molten steel, the floating velocity of inclusions increases continuously. When the drag force increases to the level equal to that of the buoyancy, the acceleration velocity of inclusions becomes zero and the floating velocity remains unchanged. According to different states of the steel, and based on the size of Re, the inclusion flow can be divided into three categories: low Re flow, intermediate flow, and high Re flow. In low Re flow, the drag force of the molten steel is Stokes [18] drag force, as shown in Eq. (1), which can also be referred to as the viscous resistance of spherical inclusions during the settling process. The drag force coefficient for the high Re flow is almost constant [19], and the drag force can be calculated from Eq. (2). The drag force coefficient for the intermediate flow can be expressed in many forms. Based on related empirical formulae, the Schiller [18] drag force expression with an error within 5% as shown in Eq. (3) is selected.

$$F_d = 6\pi\mu R v \tag{1}$$

where μ represents the steel viscosity, Pa·s; v is the floating velocity of inclusions, m/s; R denotes the inclusion radius, m; and F_d corresponds to the viscous resistance, N.

According to Eq. (1), the viscous resistance on inclusions is closely related to their velocity. The greater the movement speed of inclusions, the greater the viscous resistance, and vice versa. When the sum of gravity, buoyancy, and viscous resistance of inclusions reaches 0, the inclusion velocity does not change and the movement speed at this point is called the terminal velocity of inclusions.

$$F_d = 0.22\pi\rho_M v^2 R^2 \tag{2}$$

where ρ_M is the steel density, kg/m^3.

$$F_d = \frac{24}{\mathrm{Re}}\left(1 + 0.15\,\mathrm{Re}^{0.687}\right) \tag{3}$$

$$\mathrm{Re} = \frac{2\rho_I v R}{\mu \cdot C(Z^*)} \tag{4}$$

where ρ_I represents the inclusion density, kg/m^3; $C(Z^*)$ represents the viscosity correction coefficient, which is calculated by weight the surface area (the specific calculation formula is shown in Eq. (13)).

The inclusions reaching the terminal velocity are in the equilibrium state of multiple forces:

$$F_d = \frac{1}{2}\rho_M V^2 A C_D = F_b - F_g \tag{5}$$

where C_d represents the drag force coefficient; A represents the surface area of spherical inclusions, m^2; F_g is the gravity of

spherical inclusions, N; F_b is the steel buoyancy experienced by spherical inclusions, N.

Based on the above equations, the floating terminal velocity of inclusions under different flow conditions can be deduced, as shown in TABLE 1. The inclusion floating terminal velocity varies greatly under different flow regimes due to different drag force coefficients. Especially in the intermediate flow state, the floating velocity of inclusions is closely relevant to Re. From Eq. (4), it can be known that the inclusion size has a decisive effect on the Re when the liquid phase and the inclusion type are constant. It has been demonstrated in previous research that the size of most inclusions in die steel after rare earth treatment is less than 10 μm. Hence, the inclusion with a diameter of 10 μm is chosen as the study object for subsequent calculations.

In our model, the melting process of die steel with the addition of RE in a steel mill in Chinese is analyzed, and the main parameters are listed in TABLE 2.

By substituting the data in TABLE 2 into Eq. (4), it is determined that the flow Re of rare earth inclusions is always less than 1. Therefore, the flow state of the refining process of rare earth die steel is a low Re flow, and the drag force of molten steel belongs to the Stokes drag force. The floating terminal velocity can be calculated by:

$$v_L = \frac{2(\rho_M - \rho_I)gR^2}{9\mu} \tag{6}$$

2.2.2. Physical model of floating inclusions near MSSI

When the inclusions float to MSSI, the inclusions will interact with the interface. Inclusions are subjected to different forces such as gravity, buoyancy, viscous resistance, additional mass force, and interfacial tension. Furthermore, when the inclusions cross the interface, two different phases of molten steel and solid slag are involved, and there are dramatic transient changes in the motion of the inclusions. The physical parameters such as viscosity and density of the surrounding fluid are different at each moment, and the forces on the inclusions are closely related to these physical parameters.

Here, a parameter Z is introduced which is related to the inclusions position, and a dimensionless variable Z^* is defined to characterize the relative position of the inclusion ($Z^* = Z/R$) [22]. When the inclusion just contacts but does not interact with the interface, $Z^* = 0$; when the inclusion interacts with the interface, $0 \le Z^* \le 2$; when the inclusion leaves the liquid phase and enters the slag phase completely, $Z^* > 2$. The three processes are illustrated as Fig. 1.

When the inclusion starts to contact with the interface, the force situation of the inclusion changes, it is no longer only affected by the action of molten steel, the force is more complex. The force analysis of inclusion at MSSI is shown in Fig. 2, and the force acting on the inclusion is discussed by mathematical model.

TABLE 1

Floating terminal velocity of inclusions at different flow states

Flow state	Reynolds number Re	Drag force coefficient C_d	Calculation formula for floating terminal velocity [19]
Low Reynolds number motion	Re < 1	$\frac{24}{\mathrm{Re}}$	$v_L = \frac{2(\rho_M - \rho_I)gR^2}{9\mu}$
Intermediate flow	1 < Re < 500	$\frac{24}{\mathrm{Re}}\left(1+0.15\,\mathrm{Re}^{0.687}\right)$	$v_L = \frac{2(\rho_M - \rho_I)gR^2}{9\mu\left(1+0.15\,\mathrm{Re}^{0.687}\right)}$
High Reynolds number motion	Re > 500	0.44	$v_L = 2.46\left(\frac{\rho_M - \rho_I}{\rho_M}gR\right)^{\frac{1}{2}}$

TABLE 2

Physical parameters of molten steel and refining slag in rare earth die steel in a steel mill in China

Physical parameters	Value
Molten steel density	6500 kg/m^3
Molten steel viscosity	0.0052 Pa·s
Slag density	2500 kg/m^3
Slag viscosity	0.2004 Pa·s
Inclusion density	3990 kg/m^3
Molten steel-slag interface tension	1.384 N/m
Inclusion-molten steel interface tension	1.586 N/m
Inclusion-slag interface tension	0.44 N/m
Wettability of the three phases θ_{IMS}	0.782
Gravitational acceleration	9.8 m/s^2

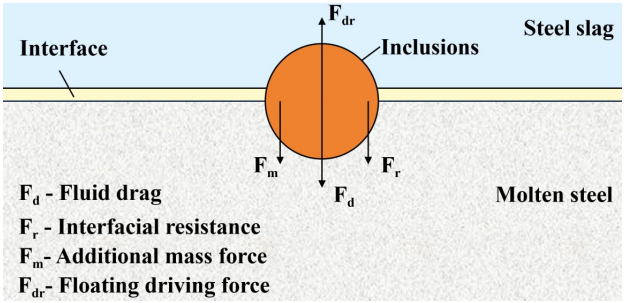

Fig. 1.

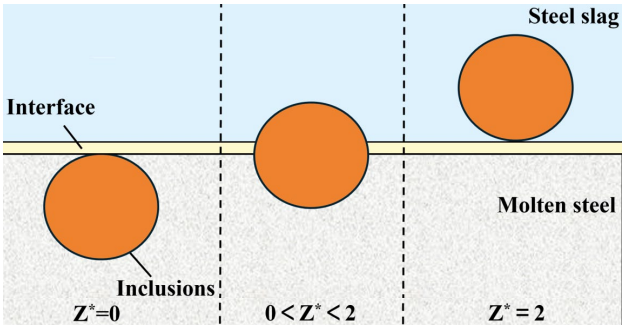

Fig. 2.

(1) Driving force of inclusion floating (difference between buoyancy and gravity) [23]

$$F_{drv} = \frac{4}{3}\pi\left(\rho_f - \rho_I\right)gR^3 \tag{7}$$

Where F_{drv} represents the driving force on the inclusion, N; ρ_f and ρ_I represent the densities of the fluid and inclusion, respectively, kg/m^3.

Because the inclusion at this time has been immersed in the steel phase and slag phase, it can be simplified as a single mixed phase. At this point, the density of the mixed fluid is recorded as ρ_f, and its value is closely related to the location of the inclusion.

$$\rho_f = \rho_s \cdot A(Z^*) \tag{8}$$

where ρ_s is the slag density, kg/m^3; $A(Z^*)$ is buoyancy variation coefficient.

According to the inclusion position, the submerged volume ratio of the inclusion between the molten steel and slag phases can be calculated, and thus the proportion of buoyancy in the two phases can be obtained. The following three equations are the submerged volume ratios of the inclusion in the molten steel and slag phases for $Z^* > 2$, $0 \le Z^* \le 2$, and $Z^* < 0$ respectively, by which the proportion of buoyancy in the two phases can be obtained.

$$A(Z^*) = \begin{cases} 1 & Z^* > 2 \\ \frac{1}{4}\left(\frac{\rho_M}{\rho_S} - 1\right)Z^{*3} - \frac{3}{4}\left(\frac{\rho_M}{\rho_S} - 1\right)Z^{*2} + \frac{\rho_M}{\rho_S} & 0 \le Z^* \le 2 \\ \frac{\rho_M}{\rho_S} & Z^* < 0 \end{cases} \tag{9}$$

Thus, the driving force of inclusion movement at the interface can be described by Eq. (10):

$$F_{drv} = \frac{4}{3}\pi\left(\rho_s \cdot A\left(Z^*\right) - \rho_I\right)gR^3 \tag{10}$$

Obviously, the position of inclusions relative to MSSI has a significant effect on the driving force.

(2) Drag force of fluid

The drag force of fluid on an inclusion is related to the relative velocity of the fluid. From the discussion in Section 1, when a RE inclusion crosses MSSI, the drag force of the molten steel belongs to the Stokes drag force [18]:

$$F_d = 6\pi\mu_s \cdot C\left(Z^*\right)Rv \tag{11}$$

In this crossing process, the inclusion is immersed in both the molten steel phase and the slag phase, and the drag force is represented by integrating the fluid friction resistance on the surface of the spherical inclusion, which represents the viscous effect with respect to the surface area. Then, the expression for characteristic viscosity can be defined as:

$$\mu = \mu_s \cdot C\left(Z^*\right) \tag{12}$$

where $C(Z^*)$ can be calculated by:

$$C\left(Z^*\right) = \begin{cases} \mu_s & Z^* > 2 \\ \left(\frac{\mu_M}{\mu_S} - 1\right)Z^{*2} - 2\left(\frac{\mu_M}{\mu_S} - 1\right)Z^* + \frac{\mu_M}{\mu_S} & 0 \le Z^* \le 2 \\ \frac{\mu_M}{\mu_S} & Z^* < 0 \end{cases} \tag{13}$$

The above three equations are the viscosity coefficient expressions for $Z^* > 2$, $0 \le Z^* \le 2$, and $Z^* < 0$, respectively, and their values are determined by the size of the surface area of the inclusion immersed in the two phases. Herein, μ_M and μ_s are the dynamic viscosity coefficients of molten steel phase and slag phase respectively, Pa·s.

(3) Additional mass force

Due to the viscous effect around the inclusion, when the inclusion accelerates or decelerates, the fluid attached to the inclusion enhances the inertia of movement, thus reducing the acceleration velocity of the inclusion. This force is the additional mass force exerted by the fluid on the inclusion. Notably, the inclusion is subjected to additional mass force only if the acceleration is not zero [24]:

$$F_M = \frac{2}{3}\pi R^3 \cdot \rho_s \cdot A\left(Z^*\right) \cdot \alpha \tag{14}$$

where α is the acceleration velocity of the inclusion, m/s^2.

α is calculated by the following equation:

$$\alpha = \frac{d^2Z}{dt^2} = \alpha^* \cdot g = \frac{d^2Z^*}{dt^{*2}} \cdot g \tag{15}$$

where α^* is the dimensionless acceleration velocity during the inclusion motion, and t^* is the dimensionless time.

t^* can be obtained by:

$$t^* = t \div \sqrt{\frac{R}{g}} \tag{16}$$

(4) Interface resistance

When an inclusion crosses MSSI, it will be hindered by the interface resistance due to the interfacial energy barrier. The interface resistance is divided into two cases according to the initial velocity when the inclusion contacts with the interface. The first case occurs when the inclusion has a relatively low initial velocity. In this case, Re < 1, and the steel film can be exhausted in a short time, so it can be assumed that the liquid film did not form. Thus, inclusions can directly contact with the slag phase, which leads to the changes of MSSI, the inclusion-steel interface, and the inclusion-slag interface at the same time. The second case is that the initial momentum of the inclusion is high, generally Re > 1. In this case, due to the large speed of inclusion, its inertia force is greater than the viscous force. In addition, because the solid inclusion is easily wetted by molten steel, it is difficult to form liquid film at MSSI during the separation process. Based on the above analysis, our proposed model does not consider the influence of liquid film on the interface resistance.

The expression for the interface resistance without liquid film is:

$$F_r = \frac{dE_r}{dZ} \tag{17}$$

where F_r is the interface resistance on the inclusion, N; E_r is the interfacial energy, J.

The interfacial energy change consists of three parts as follows:

$$E_r = -\pi\left(2R_I Z - Z^2\right)\sigma_{MS} + 2\pi R_I Z\sigma_{SI} + \\ + 2\pi R_I(2\pi R_I - Z)\sigma_{IM} \tag{18}$$

where σ_{MS}, σ_{SI}, and σ_{IM} are the interfacial tension coefficients of the steel-slag interface, inclusion-slag interface, and inclusion-steel interface respectively, N/m.

The interface resistance can be determined by [25]:

$$F_r = \frac{dE_r}{dZ} = 2\pi R_I \sigma_{MS} B\left(Z^*\right) \tag{19}$$

Herein,

$$B\left(Z^*\right) = Z^* - 1 - \cos\theta_{IMS} \tag{20}$$

where θ_{IMS} represents the wetting angle formed between the three phases, B(Z*) is the interfacial tension variation coefficient.

$$\cos\theta_{IMS} = \frac{\sigma_{IM} - \sigma_{IS}}{\sigma_{MS}} \tag{21}$$

According to Eqs. (17)-(21), the wetting angle θ_{IMS} has a big effect on the process of inclusion passing through MSSI without liquid film. If $\theta_{IMS} < 0$, then in the two phases, the slag phase has better inclusion wettability than the molten steel phase; if $\theta_{IMS} > 0$, then the slag phase has poorer inclusion wettability than the molten steel phase. Therefore, in the absence of liquid film, the wettability between the three phases plays a very significant role in the process of the inclusion passing through the interface.

3. Mathematical model of inclusion motion

The process of the inclusion passing through MSSI can be divided into two distinct stages. The first stage of momentum accumulation before the inclusion comes into contact with MSSI and the second stage when the inclusion continues to rise after coming into contact with MSSI. The mathematical models of the above two stages are analyzed and discussed in the following.

3.1. Mathematical model of inclusion floating in molten steel

The floating movement of inclusion in molten steel is the momentum accumulation stage before it passes through MSSI, that is, the initial stage. This stage determines the initial physical quantity of the inclusion as it passes through the interface. According to previous analysis, the forces exerted on inclusion in molten steel phase include buoyancy, gravity, drag force, and additional mass force. From Newton's second law, the following equation can be obtained:

$$F_I = F_{drv} - F_d - F_m = \frac{4}{3}\pi {R_I}^3 \cdot \rho_I \cdot \alpha \tag{22}$$

where F_I is the resultant force on the inclusion, N.

According to Eq. (11), the drag force of the inclusion is related to its flow state. The inclusion in low Re flow, intermediate flow, and high Re flow is subject to different drag forces, which affects its upward movement. The flow state of low Re flow will be discussed in detail below.

According to Eqs (10), (11), and (14), the expressions for driving force, drag force, and additional mass force on inclusion in the molten steel can be obtained. Substituting these expressions into Eq. (22) yields:

$$\alpha = \frac{\frac{4}{3}\pi R^3\left(\rho_M - \rho_I\right)g - 6\pi\mu_M Rv}{\frac{4}{3}\pi R^3\left(\rho_I + \frac{1}{2}\rho_M\right)} \tag{23}$$

The relationship between velocity and acceleration velocity is given by:

$$v_t = v_{t-dt} + \alpha \cdot dt \tag{24}$$

where v_t and v_{t-dt} are the inclusion velocities at t and $t-dt$ respectively, m/s.

Substituting Eq. (23) into Eq. (24) yields:

$$v_t = \frac{\frac{4}{3}\pi R^3 (\rho_M - \rho_I) g \cdot dt + \frac{4}{3}\pi R^3 \left(\rho_I + \frac{1}{2}\rho_M\right) v_{t-dt}}{\frac{4}{3}\pi R^3 \left(\rho_I + \frac{1}{2}\rho_M\right) + 6\pi\mu_M R \cdot dt} \tag{25}$$

Thus, the inclusion displacement can be obtained by summing the cumulative number of inclusion movement in each dt moment:

$$S = \sum \frac{v_t + v_{t-dt}}{2} dt \tag{26}$$

3.2. Mathematical model of inclusion passing through MSSI

Based on the previous analyses of the interfacial resistance when the inclusion pass through MSSI, it can be known that the resultant force acting on the inclusion is significantly different in the presence and absence of a liquid film. In the following, we take the resultant force model without liquid film hypothesis as an example for analysis. According to Newton's second law, the resultant force of inclusion passing through MSSI is given by:

$$F_I = F_{drv} - F_d - F_m - F_r = \frac{4}{3}\pi {R_I}^4 \rho_I g \frac{d^2 Z^*}{dt^{*2}} \tag{27}$$

Substituting Eqs. (10), (11), (14), and (19) into Eq. (27) and transforming them into dimensionless variables yield:

$$\frac{d^2 Z^*}{dt^{*2}} = 2\frac{\rho_s A\left(Z^*\right) - \rho_I}{\rho_s A\left(Z^*\right) + 2\rho_I} - 3D\left(Z^*\right) B\left(Z^*\right) - \frac{9}{E\left(Z^*\right)} C\left(Z^*\right) \frac{dZ^*}{dt^*} \tag{28}$$

where

$$D\left(Z^*\right) = \frac{\sigma_{MS}}{{R_I}^2 g\left(\rho_s A\left(Z^*\right) + 2\rho_I\right)} \tag{29}$$

$$E\left(Z^*\right) = \frac{\sqrt{{R_I}^3 g}\left(\rho_s A\left(Z^*\right) + 2\rho_I\right)}{\mu_s} \tag{30}$$

When the initial position and initial velocity of the inclusion are determined, Eq. (28) can be solved to obtain the inclusion displacement at a certain moment in the precess of the inclusion passing through MSSI. It should be noted that the applicability of this equation is strictly limited to conditions where Re < 1.

4. Influencing factors for inclusion passing through MSSI

Based on numerical simulation [26], water modelling experiments [27], and in-situ observations [28], a series of new insights into the influences of various physical properties on the inclusion removal process have been developed. In general, the physical properties of steel constituents are relatively stable and do not change much during refining and continuous casting, so they have little influence on the inclusion removal process. By contrast, the physical properties of inclusion and slag have a significant effect on the removal of inclusion. Hence, in this section, we will focus on investigating the influences of physical parameters of inclusion and slag on inclusion passing through MSSI.

4.1. Influences of physical parameters on inclusions passing through MSSI

The motion model of inclusions near MSSI derived from the above analysis shows that the physical parameters of inclusions have a big impact on the removal of inclusions. On the one hand, the size of inclusions affects the flow state of inclusions in molten steel, and then affects the floating terminal velocity of inclusions. On the other hand, the size of inclusions also affects the motion process when it crosses MSSI, as indicated by Eq. (22).

Fig. 3 shows the influences of inclusion size on inclusion displacement. The RE inclusions with diameters of 1, 5, and 10 μm are selected and substituted into our proposed model. It can be seen from Fig. 3 that after the inclusion is in contact with the molten steel-slag interface, it constantly breaks through the interface and moves towards the slag phase (When the migration displacement reaches 2R, it indicates that the inclusions have completely entered the slag phase.). After reaching the position of 1.82R, the inclusions stabilize and finally stay at this position. According to the analysis results, the three rare earth inclusions with different diameters finally stay at the same

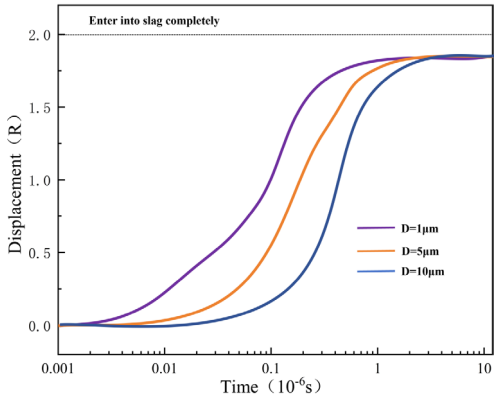

Fig. 3.

position, indicating that smaller rare earth inclusions (less than 10 μm in diameter) do not have a significant impact on their maximum displacement through MSSI. However, the size of inclusion affects their time of breaking through MSSI; the bigger the size, the longer the time.

In this study, the density of rare earth inclusions was selected as 3990 kg/m^3. To elucidate the influences of inclusion density on the maximum displacement of inclusion crossing MSSI, two groups of rare earth inclusion density under different slag systems produced by the same steel mill are chosen for comparison, and the results are shown in Fig. 4.

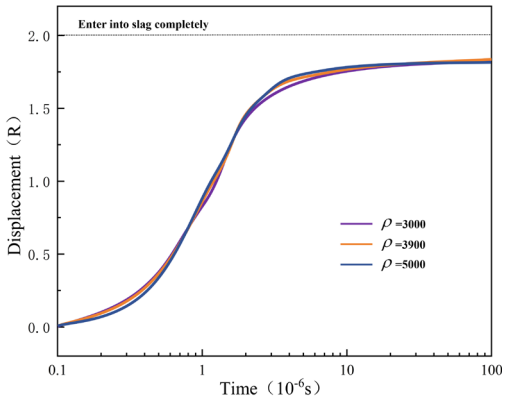

Fig. 4.

In the calculations, three different inclusions with densities of 3000, 3990, and 5000 kg/m^3 are involved, and the inclusions have a diameter of 10 μm. Seen from Fig. 4, the maximum displacement of inclusions at MSSI remains unchanged although the density of inclusions increases from 3000 to 5000 kg/m^3, indicating that the inclusion density had no significant influence on its maximum displacement. In fact, no matter in slag, molten steel, or MSSI, when the inclusion density is larger, the driving force will be smaller, and the corresponding maximum displacement of inclusions should be smaller. In the calculations process, for inclusions with a diameter less than 10 μm, although the density of inclusions varies greatly, due to its relatively small size, the driving force to disrupt the equilibrium state of the inclusions at MSSI is insufficient. Therefore, the influence of inclusion density on its maximum displacement is small and can be ignored.

4.2. Influences of physical parameters of slag on inclusions passing through MSSI

The physical parameters of slag also have a big impact on the removal of inclusions at the interface, which can be adjusted by adjusting the characteristics of slag, mainly changing the viscosity and surface tension coefficient slag. During the production process of die steel, the composition of slag changed with the melting process, and the interfacial tension between slag and molten steel changes with the composition of slag. As shown in Eq. (19), the interface resistance of inclusions is related to the molten steel-slag interfacial tension σ_{MS}.

The slag system selected in this study is a rare earth slag system with composition of (CaF_2-Al_2O_3-CaO-MgO-Ce_2O_3), and the given range of molten steel-slag interfacial tension σ_{MS} is 1.332~1.433 N/m. In order to analyze the influencing rules of MSSI tension on the displacement of inclusions, a comparative analysis was also conducted on two sets of rare earth inclusion MSSI under different slag systems. 1.33, 1.38, and 1.43 N/m were selected for numerical simulation calculations, and Fig. 5 shows the calculation results (the diameter of inclusions is 10 μm). Seen from Fig. 5, when the interfacial tension is changed, the inclusion motion behavior does not change, and the inclusions do not enter the slag layer completely. However, as MSSI tension increases from 1.33 to 1.43 N/m, the final stable displacement of inclusions presents an obviously decreasing trend.

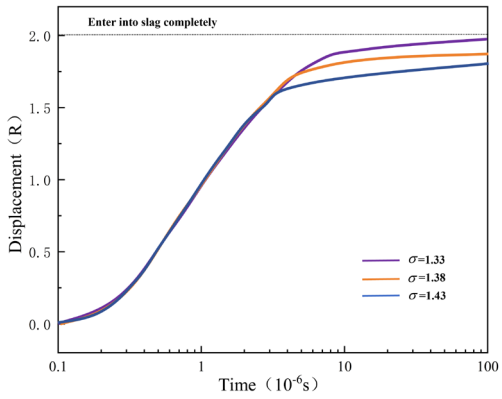

Fig. 5.

Next, we will discuss the influence of slag density on the displacement and breakthrough time of inclusions. Still select inclusions with a diameter of 10 μm for calculation. When other slag parameters are fixed, the slag is assigned with different densities of 2000, 2500, and 3000 kg/m^3 respectively for numerical simulation calculations, and the obtained curves are almost the same as those in Fig. 4. Hence, the relationship between displacement and time of inclusions at the interface basically remains unchanged, and the slag density has little influence on the movement behavior of inclusions at the interface.

5. Conclusions

In this work, the movement behavior of RE inclusions in die steel under RE slag system at MSSI was analyzed by mathematical model.

(1) The floating movement of RE inclusions in molten steel belongs to Stokes flow. The Re affects the terminal floating velocity during the floating process, and the terminal floating velocity determines the initial velocity of the inclusions passing through MSSI.

(2) The size of inclusion affects the time it takes to break through MSSI, and the two are positively correlated. The influence of the size and density of the inclusion on its maximum displacement through MSSI is not significant.

(3) The MSSI tension significantly affects the removal of inclusion at the interface; the larger the tension, the smaller the displacement of inclusion passing through the interface, and the more difficult of its passing through the interface. In addition, the effect of slag density on the inclusion passing through the interface is not obvious.

Acknowledgments

This work was supported by the National Natural Science Foundation of China (Nos. 52364044, 52204364, and 52264045), Scientific Research Special Project for First-Class Disciplines of Education Department of Inner Mongolia Autonomous Region (Nos. YLXKZX-NKD-001 and YLXKZX-NKD-011), Central Guidance on Local Science and Technology Development Fund Projects of Inner Mongolia Autonomous Region (No. 2022ZY0090), and Basic Scientific Research Business Expenses of Colleges and Universities of Inner Mongolia Autonomous Region (No. 2023QNJS011).

REFERENCES

[1] L. Chen, W. Chen, Y. Hu, Z. Chen, Y. Xu, W. Yan, Effect of Al antioxidant in MgO-C refractory on the formation of Al_2O_3-rich inclusions in high-carbon steel for saw wire under vacuum conditions. Ironmak. Steelmak. **45**, 272-279 (2018).

[2] C.G. Aneziris, S. Dudczig, J. Hubálková, M. Emmel, G. Schmidt, Alumina coatings on carbon bonded alumina nozzles for active filtration of steel melts. Ceram. Int. **39**, 2835-2843 (2013).

[3] H.L. Yang, P. He, Y.C. Zhai, Removal Behavior of Inclusions in Molten Steel by Bubble Wake Flow Based on Water Model Experiment. ISIJ Int. **54**, 578-581 (2014).

[4] S. Michelic, J. Goriupp, S. Feichtinger, Y.B. Kang, Study on Oxide Inclusion Dissolution in Secondary Steelmaking Slags Using High Temperature Confocal Scanning Laser Microscopy. Steel. Res. Int. **87**, 57-67 (2016).

[5] K. Nakajima, K. Okamura, Inclusion transfer behavior across molten steel-slag interface. 4th International Conference on Molten Slags and Fluxes. 505-510 (1992).

[6] J. Strandh, K. Nakajima, R. Eriksson, P. Jönsson, A mathematical model to study liquid inclusion behavior at the steel-slag interface. ISIJ Int. **45**, 1838-1847 (2005).

[7] J. Strandh, K. Nakajima, R. Eriksson, P. Jönsson, Solid inclusion transfer at a steel-slag interface with focus on tundish conditions. ISIJ Int. **45**, 1597-1606 (2005).

[8] S.F. Yang, W. Liu, J.S. Li, Motion of solid particles at molten metal-liquid slag interface. JOM. **67**, 2993-3001 (2015).

[9] S.F. Yang, J.S. Li, C. Liu, L.Y. Sun, H.B. Yang, Motion behavior of nonmetal inclusions at the interface of steel and slag, Part II: model application and discussion. Metall. Mater. Trans. B **45**, 2453 (2014).

[10] X. Tao, J. Cao, J. Wang, X. He, L. Meng, Y. Guo, T. Wang, D. Li, J. Fan, C. Chen, Physical model of inclusions removal at static steel-slag interface. Materials **17**, 2244(2024).

[11] Y.L. Zhou, Z.Y. Deng, M.Y. Zhu, Study on the separation process of non-metallic inclusion at steel-slag interface using water modeling. Int. J. Min. Met. Mater. **24**, 627-637 (2017).

[12] J. Cao, Y. Li, W. Lin, J. Che, F. Zhou, Y. Tan, D. Li, J. Dang, C. Chen, Assessment of inclusion removal ability in refining slags containing Ce_2O_3. Crystals **13**, 202 (2023).

[13] C. Liu, R.I. Revilla, Z. . Liu, D.W. Zhang, X.G. Li, H. Terryn, Effect of inclusions modified by rare earth elements (Ce, La) on localized marine corrosion in Q460NH weathering steel. Corros. Sci. **129**, 82-90 (2017).

[14] X.J. Liu, C.Q. Yang, H.P. Ren, Y.M. Li, Z.L. Jin, F. Zhang, J.C. Yang, Origin mechanism of pitting corrosion induced by cerium inclusions. J. Rare Earths **41**, 1448-1458 (2023).

[15] J. Wang, L.Z. Wang, C.R. Li, Y.Q. Zhai, Agglomeration behavior of rare earth inclusions and alumina inclusions at the interface between argon and molten steel. J. Rare Earths **41**, 2033-2044 (2023).

[16] X. Li, Z.H. Jiang, X. Geng, M.J. Chen, L.Z. Peng, Evolution Mechanism of Inclusions in H13 Steel with Rare Earth Magnesium Alloy Addition. ISIJ Int. **59**, 1552-1561 (2019).

[17] X.Q. Wang, Z.W. Wu, B. Li, W.X. Chen, J. Zhang, J. Mao, Inclusions modification by rare earth in steel and the resulting properties: A review, J. Rare Earths **42**, 431-445 (2024).

[18] D.A. Rupp, L.F. Mortimer, M. Fairweather, Stokes number and coupling effects on particle interaction behavior in turbulent channel flows. Phys. Fluids **35**, 113307 (2023).

[19] D. Chandran, A. Zampiron, A. Rouhi, M.K. Fu, D. Wine, B. Holloway, A.J. Smits, I. Marusic, Turbulent drag reduction by spanwise wall forcing. Part 2. High-Reynolds-number experiments. J. Fluid Mech **968**, A7 (2023).

[20] W.H. Liu, Y.P. He, M.Z. Li, C. Huang, Effect of drag models on hydrodynamic behaviors of slurry flows in horizontal pipes. Phys. Fluids **34**, 103311 (2022).

[21] C. Liu, S.F. Yang, J.S. Li, L.B. Zhu, X.G. Li, Motion Behavior of Nonmetallic Inclusions at the Interface of Steel and Slag. Part I: Model Development, Validation, and Preliminary Analysis. Metall. Mater. Trans. B **47**, 1882-1892 (2016).

[22] M.J. Dalbe, R. Juanes, Morphodynamics of Fluid-Fluid Displacement in Three-Dimensional Deformable Granular Media. Phys. Rev. Appl. **9**, 024028 (2018) .

[23] D. Bouris, G. Bergeles, Investigation of inclusion re-entrainment from the steel-slag interface. Metall. Mater. Trans. B **29**, 641-649 (1998).

[24] L.T. Wang, Q.Y. Zhang, S.H Peng, Z.B. Li, Mathematical Model for Growth and Removal of Inclusion in a Multi-tuyere Ladle during Gas-stirring. ISIJ Int. **45**, 331-337 (2005).

[25] M. Valdez, G.S. Shannon, S. Sridhar, The Ability of Slags to Absorb Solid Oxide Inclusions. ISIJ Int. **46**, 450-457 (2006).

[26] W. Liu, S.F. Yang, J.S. Li, Calculation of Static Suspension Depth and Meniscus Shape of a Solid Spherical Inclusion at the Steel-Slag Interface. Metall. Mater. Trans. B **51**, 422-425 (2020).

[27] J.W. Cho, H.G. Lee, Cold Model Study on Inclusion Removal from Liquid Steel Using Fine Gas Bubbles. ISIJ Int. **41**, 151-157 (2001).

[28] M. Jiang, X.H. Wang, J.J. Pak, P. Yuan, In Situ Observation on Behaviors of CaO-MgO-Al_2O_3-SiO_2 Complex Inclusions at Solid-Liquid Interface of Low-Oxygen Special Steel. Metall. Mater.Trans. B **45**, 1656-1665 (2014).